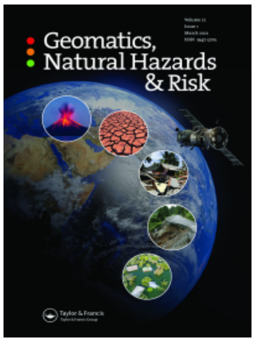


Geomatics, Natural Hazards and Risk

ISSN: (Print) (Online) Journal homepage: www.tandfonline.com/journals/tgnh20

# Characterization of flood and drought hazards on the Gereb-Geba water supply dam in the semi-arid northern Ethiopian highlands

Henok Shiferaw, Amanuel Zenebe, Eyasu Yazew, Biniyam Yisak, Atkilt Girma, Muez Araya, Gebreyohannes Zenebe & Alessandra Giannini

**To cite this article:** Henok Shiferaw, Amanuel Zenebe, Eyasu Yazew, Biniyam Yisak, Atkilt Girma, Muez Araya, Gebreyohannes Zenebe & Alessandra Giannini (2024) Characterization of flood and drought hazards on the Gereb-Geba water supply dam in the semi-arid northern Ethiopian highlands, Geomatics, Natural Hazards and Risk, 15:1, 2290846, DOI: 10.1080/19475705.2023.2290846

**To link to this article:** https://doi.org/10.1080/19475705.2023.2290846



Published online: 18 Dec 2023.

GEOMATICS, NATURAL HAZARDS AND RISK
2024, VOL. 15, NO. 1, 2290846
https://doi.org/10.1080/19475705.2023.2290846



# Characterization of flood and drought hazards on the Gereb-Geba water supply dam in the semi-arid northern Ethiopian highlands

Henok Shiferaw[a,b], Amanuel Zenebe[b,c], Eyasu Yazew[a,c], Biniyam Yisak[b]*, Atkilt Girma[b,c], Muez Araya[d], Gebreyohannes Zenebe[b] and Alessandra Giannini[e,f]

[a]Institute of Water and Environment, Mekelle University, Mekelle, Ethiopia; [b]Institute of Climate and Society, Mekelle University, Mekelle, Ethiopia; [c]Department of Land Resources Management and Environmental Protection, Mekelle University, Mekelle, Ethiopia; [d]Department of Dam and Infrastructure Construction, Tigray Water Works Construction Enterprise, Mekelle, Ethiopia; [e]Laboratoire de Météorologie Dynamique/IPSL, Ecole Normale Supérieure, PSL Research University, Sorbonne Université, Ecole Polytechnique, IP Paris, CNRS, Paris, France; [f]International Research Institute for Climate and Society (IRI), Columbia University, Palisades, NY, USA

**ABSTRACT**

Evaluating the flood and drought hazards provides vital information for sustainable water resources management, particularly in semi-arid, water-deficit environments. Most prior studies were limited in exploring the flood and drought hazards, which are important for early warning systems and preparedness. This study characterized the hydrological extreme hazards on the Gereb-Geba reservoir, namely the Suluh, Genfel, and Agula rivers. Flood frequency analysis was performed using the fitted flood frequency distribution in MATLAB. The 2D hydrodynamic model HEC-RAS was implemented to produce a flood-inundation map. Meteorological, agricultural, and hydrological droughts were analyzed using the Standardized Precipitation Index (SPI), Vegetation Condition Index (VCI), and Streamflow Drought Index (SDI), respectively. Using the Generalized Extreme Value (GEV), the estimated flood magnitude showed an increasing tendency in all the rivers across all the return periods (2-, 5-, 10-, 20-, 50-, and 100-years). The reservoir inundated an area of 12.8 $km^2$ at an elevation of 1830 m.a.s.l. with a water depth of 80 m at the outlet. Suluh experienced more severe to extreme hydrological drought episodes than the Agula and Genfel rivers. Severe to extreme meteorological droughts were also observed in the respective catchments. Moreover, severe agricultural drought prevalence was also detected across all the river catchments. This study provides vital and comprehensive flood and drought information for water resources planning, management, and development.

**ARTICLE HISTORY**
Received 14 June 2023
Accepted 29 November 2023

**KEYWORDS**
Agricultural drought; flood; hydrological drought; meteorological drought; Northern Ethiopia

CONTACT Amanuel Zenebe amanuelzenbe@gmail.com
*Biniyam Yisak is also affiliated to Department of Atmospheric Sciences, National Taiwan University, Taipei, Taiwan, and Earth System Science, Taiwan International Graduate Program (TIGP), Academia Sinica.

## 1. Introduction

The occurrence of extreme events in the hydrological cycle is a priority concern of hydrologists, policymakers, and water managers in the twenty-first century. Flood and drought events are a major global concern, as these events have major economic, environmental, and social impacts (World Economic Forum 2017; Wang et al. 2020). The extent of societal impact and economic damage may vary across countries.

Recent studies show that East Africa is one of the most vulnerable regions to extreme events (Gebrechorkos et al. 2019; Gebremeskel Haile et al. 2019). The extreme events cause widespread flooding and rapid and prolonged increases in the levels of many lakes, resulting in significant economic disruption in the region (Mbungu et al. 2012). Extreme events cause loss of life, damage to dwellings and vulnerable rural infrastructure, and agricultural and industrial production losses. This situation underscores the need for careful understanding of the causes of hydrological extremes for the appropriate design and management of water resource systems in the region. It is essential to characterize the floods and droughts to reduce their negative hazard impacts and risks. Structural measures, such as dikes, levees, embankments, and dams, have been used to reduce the potential hazards. Also, subsurface storage has been harnessed historically as a buffer for flood and drought hazards (Markantonis et al. 2018).

Flood and hydrological drought do not have any uniform and broadly agreed definitions. For this purpose, we adopted the following definitions: For a given area over a given period, flood is the high-flow, and it occurs when the amount of water at a specific site surpasses a threshold value (Kundzewicz and Kaczmarek 2009). Similalry, hydrological drought is the low-flow, whereby available water lies below a threshold value (Wilhite 2000; Tallaksen and Van Lanen 2004).

Climate change worsens floods and droughts. It is expected to alter the hydrological cycle, leading to an increased risk and frequency of droughts and floods (Gebrechorkos et al. 2023). The hydrological cycle changes with global warming, which likely increases the intensity of extreme precipitation events and the risk of flooding and drought (Tabari 2020; Yin et al. 2021). This imposes heavy costs on aquatic and terrestrial ecosystems, human societies, and the economy (Yin et al. 2022, 2023).

Since there is great concern about hydrological extremes in the world, the subject is rigorously investigated (e.g. Zhang et al. 2014; Ekolu et al. 2022). Despite several studies conducted in different places, very little is known about the temporal characteristics of hydrological extremes for different climatic regimes across Ethiopia. The few studies conducted have focused on the temporal variability of either high or low flows in different basins (Awass 2009; Melesse et al. 2010; Seyoum et al. 2013). Many of the earlier hydrological extreme studies focused on the statistical separation of historic data flow as high or low or on detecting trends and abrupt changes. They are limited to investigating the intensity, duration, frequency, onset, and cessation parameters. Investigating these parameters is important for water resource planning, management, and development.

Generally, the aforementioned studies in Ethiopia have been focused on other parts of the country, including the Blue Nile, Baro-Akobo, Wabi Shebele, and Omo basins.

However, in the headwaters of the Tekeze-Atbara River Basin, in the semi-arid northern highlands of the country, where such evidence is arguably most needed, there have been limited comprehensive investigations. The basin has exhibited a significant change in streamflow over the last three decades (Gebremicael et al. 2016; Tesfaye et al. 2017; Shiferaw et al. 2018). Raising the concern that the streamflow at the study site is non-stationary, the situation calls for the need to study the temporal characteristics of the streamflow for planning and management purposes.

Floods and droughts are more evident in arid and semi-arid regions where water availability is scarce and limited (Byakatonda et al. 2018b). This is the case in the headwater river catchments where this study is carried out, which have erratic and intense rainfall usually concentrated during the main rainy season, from June to September. Intense rainfall combined with the steep topography can create a different magnitude of floods and recurrent droughts, which affect the hydrological regime of the river catchments. Coping with extreme hydrological events, particularly floods and droughts, requires putting in place different reservoir operations and development strategies (McMartin et al. 2018; Ridolfi et al. 2019). In line with this need, at the study site, a water supply dam called Gereb-Geba is currently under construction. The dam is expected to provide water supply for drinking purposes to the capital of Tigray, Mekelle, which is the second most populous city after Ethiopia's capital, Addis Ababa. The water supply dam is a large project that demands an estimated cost of 305 million US dollars. Given the significant investment, it is necessary to periodically revise research studies for monitoring and evaluation purposes. In this regard, our study provides scientific evidence for policymakers and practitioners to make the informed decisions needed for the water supply dam to serve its purpose. In addition to this practical need, this study also serves the purpose of validating the streamflow drought index (SDI) in topographic and climatic settings not previously considered (Nalbantis and Tsakiris 2009). SDI is reasonably validated in different parts of temperate and tropical regions, for example, in Greece (Nalbantis and Tsakiris 2009), in Turkey (Altin et al. 2019), and in Brazil (Melo et al. 2016). However, it has not been validated as much in semi-arid basins and catchments such as the Gereb-Geba river catchments, which are characterized by a complex topographic landscape and hydrological system. Furthermore, it is vital to understand the other types of drought, such as agricultural and meteorological drought, for the purpose of sustainable water resource management. For all these reasons, this research aimed to characterize the extreme hydrological events—flood, hydrological, meteorological, and agricultural drought hazards—in the semi-arid headwaters of the Gereb-Geba river catchments in the northern Ethiopian highlands.

## 2. Materials and methods

### 2.1. Study area

The study site is located in the upper headwater of the Tekeze-Atbara River basin, Geba catchment, in the Tigray regional state, in the northern Ethiopian highlands (Figure 1). It lies between latitudes 13°20′49″ and 14°10′13″ North, longitudes

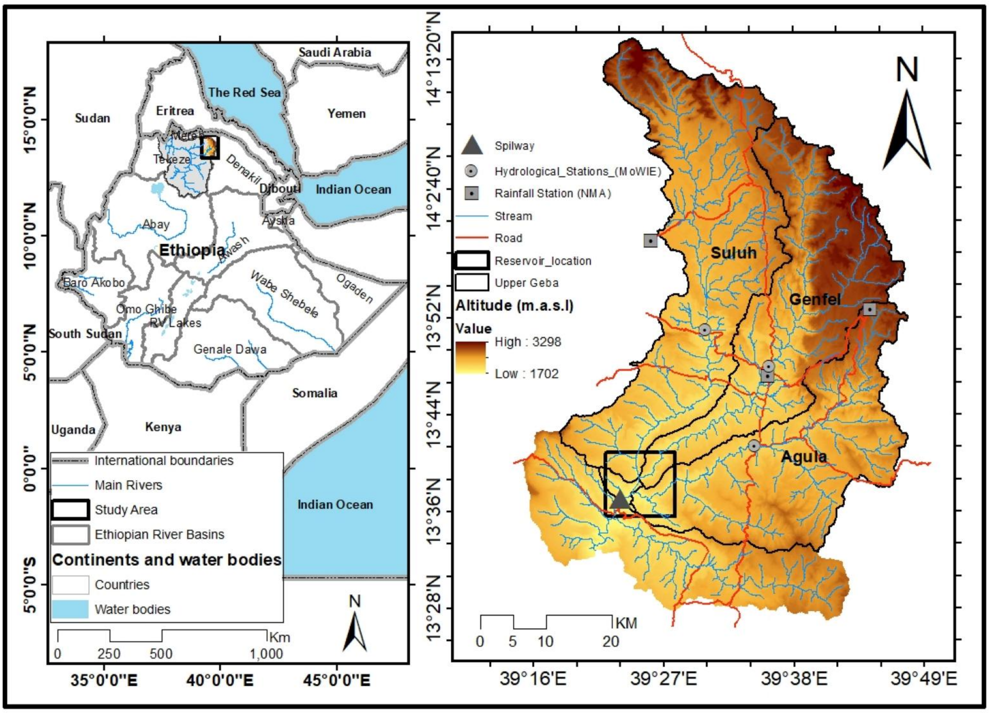


Figure 1. Location map of the Gereb-Geba reservoir water supply project in the headwaters of the Tekeze-Atbara River Basin.

between 39°21′00″ and 39°46′30″ East, and at altitudes ranging from 1744 to 3298 meters above sea level (Figure 1).

Rainfall in the Geba catchment is bimodal, with a short rainy season occurring between February and April and a long-rainy season from June to September. Rainfall is highly variable in space and time, with mean annual rainfall ranging between 520 mm and 630 mm (NMA 2021). The mean annual temperature ranges between 16 and 20 °C (NMA 2021). The area consists of cropland (39.2%), bush and shrub covered areas (30%), forest land (1.5%), plantations (3.81%), grassland (7%), woodland (6%), bare land (11%), urban areas (0.94%), and water bodies (0.24%) (Gebremicael et al. 2019).

## 2.2. Reservoir physical characteristics

The reservoir dam site is situated at the trunk of the Geba River, and it is a U-shaped valley (see Figure 2). There are three major tributaries in the upper reaches of the reservoir dam, namely Suluh, Genfel, and Agula. The total catchment area is 2,540 km$^2$, and, a maximum storage capacity of the reservoir is 363 million m$^3$ of water.

The dam (earthen) is a clay-core dam with a top crest width of 8 m, and elevation of 1830 m, and a maximum dam height of 80 m. The structures of the headworks include a dam, spillway, intake tower, bottom outlet, headrace pipeline from the

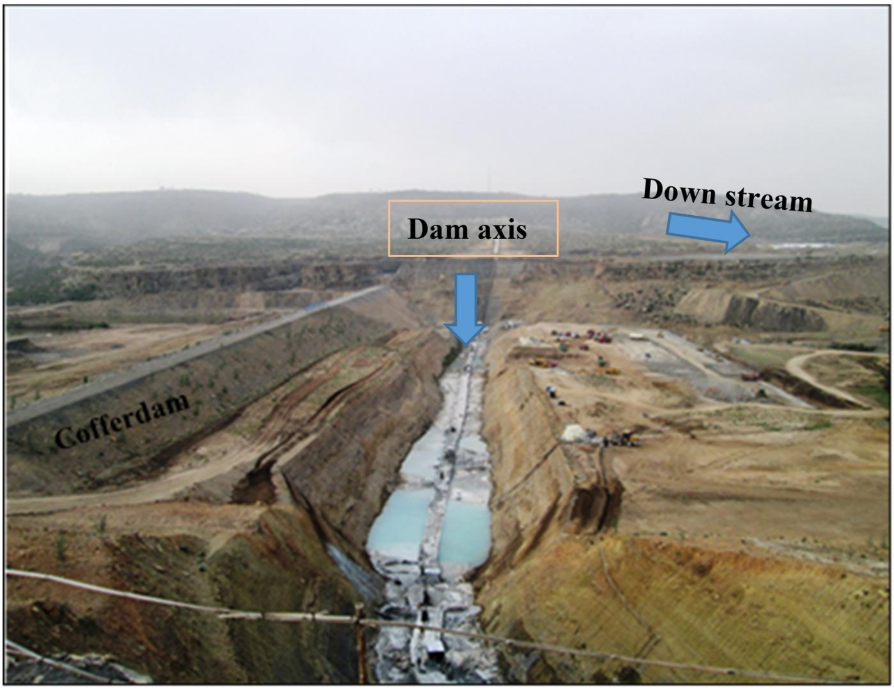


Figure 2. The Gereb-Geba water supply dam project (currently under construction) is located in the Geba catchment, 20 kilometers west of Mekelle, Ethiopia. The project is intended to meet municipal water needs in Mekelle.

water intake to the water plant, and a water treatment plant. The general lithology of the reservoir area is mainly composed of Mesozoic, Cenozoic sedimentary, and volcanic rock.

### 2.3. Datasets

The daily rainfall station data (1980-2017) for Atsbi, Wukro, and Hawezn were collected from the Ethiopian National Meteorological Agency (NMA). Besides, the daily streamflow data (1992-2014) for the gauge stations of the Suluh, Genfel, and Agula rivers were collected from the Ethiopian Ministry of Water, Irrigation and Energy (MoWIE) gauge station records. A fourth ungauged river (Matgala) also flows into the reservoir. Matgala is ungauged. The monitoring (guage) stations are not well located at the outlet of the catchments (Figure 1). As a result, a considerable portion of the catchments below the gauging stations were not covered. The area that is not covered by the gauging stations contributes significantly to the volume of the flow. Considering this, we quantified the missing magnitude of the flow for each catchment using a statistical relationship between catchment area and streamflow, as suggested by Zenebe et al. (2013), who considered ten other sub-catchments in the study site and its surrounding areas. Following this, we are able to compute the total river flow from each catchment area below the gauging stations for the area of Suluh (340 $km^2$), Genfel (224 $km^2$) and Agula (255 $km^2$) catchments, respectively.

For the purpose of this study, since there was no available streamflow data after 2015, our flood and hydrological drought analyses were limited to 1992 - 2014 period. Daily rainfall station data (1980-2017) for Atsbi, Wukro, and Hawezn were collected from the NMA. The missing data records were filled using a rainfall satellite product of Climate Hazards Group InfraRed Precipitation with Stations (CHIRPS v2.0). Atsbi station represented Agula catchment, Wukro for Genfel, and Hawzen for Suluh catchment, respectively. We also used a 30-meter- resolution Digital Elevation Model (DEM) from the Shuttle Radar Topographic Mission (SRTM) to compute the volume of water stored and flood inundation in the reservoir. The DEM was able to generate the TIN to develop the river cross-section or river geometry using the HEC-GeoRAS model. The 250-meter spatial resolution eMODIS-NDVI (2003-2017) datasets used to analyze the agricultural drought of the study site were downloaded from the USGS database (https;//earthexplorer.usgs.gov/).

## 2.4. Data analysis

### 2.4.1. Flood frequency analysis

Due to the non-stationary nature of the streamflow at the study site, we implemented flood frequency analysis. High-flow values were separated from historical data using the 7-day Daily Annual Maximum (DAM) approach using Indicators of Hydrologic Alteration (IHA). In this study, we considered four probability distribution types for flood frequency analysis: Generalized extreme value (GEV), Gumbel (EV1), Log-Pearson (P3), and Gamma. The mathematical details are provided in Equations 1-4. We tested each distribution type to select the best-fit distribution for each river, using the functionality available in MATLAB version R2016a.

*2.4.1.1. Generalized extreme values (GEV).* The GEV distribution is a family of continuous probability distributions that combines the Gumbel (EV1) and Weibull distributions. The GEV distribution makes use of three parameters: location $(\xi)$, scale $(\alpha)$ and shape $(k)$ (Salinas et al. 2014). The parameters are estimated by the method of moments. The probability distribution function (pdf) is calculated using Equation 1:

$$f_{\xi,\mu,\sigma}(x) = \frac{1}{\sigma}\left(1+\xi\frac{(x+\mu)}{\sigma}\right)^{1-1/\xi} \exp\left(-\left(1+\xi\frac{(x+\mu)}{\sigma}\right)^{-1/\xi}\right) \quad \xi \neq 0 \tag{1}$$

*2.4.1.2. Gumbel (EV1).* Gumbel is an extreme value (EV) distribution; thus, Extreme value type-I corresponds to the Gumbel distribution, and the probability distribution is given as Equation 2:

$$f(x) = \frac{1}{\alpha}\exp\left[-\frac{x-\mu}{\alpha} - \exp\left(-\frac{x-\mu}{\alpha}\right)\right] \tag{2}$$

where, $\alpha$ -scale and μ-shape, are the parameters of the Gumbel distribution, estimated by the L-moment.

*2.4.1.3. Log-Pearson (3P).* The Log-Pearson (3P), another function of the gamma family of Probability Distribution Models (PDM), defines a random variable, and logarithm follows the Log Pearson Type III PDM. The pdf and cdf of Log-Pearson (3P) are as follows in Equation 3:

$$f(x) = \frac{1}{|\alpha|\Gamma(\beta)} \int_{\xi}^{x} \left[ \left( \frac{x-\xi}{\alpha} \right)^{\beta-1} \right] \exp\left[ -\frac{(\ln(x)-\xi)}{\alpha} \right] dx \tag{3}$$

Where, $\beta$ is shape $\alpha$ is scale, and $\xi$ is location parameters

*2.4.1.4. Gamma (3P).* The other regularly used probability distribution function in extreme event studies is the Gamma (3P) PDM, which is a 2-parameter Gamma distribution with a third parameter for the location. The pdf of Gamma (3P) is defined as presented in Equation 4:

$$f(x) = \frac{1}{|\alpha|\Gamma(\beta)} \int_{\xi}^{x} \left[ \left( \frac{x-\xi}{\alpha} \right)^{\beta-1} \right] \exp\left[ -\frac{(x-\xi)}{\alpha} \right] dx \tag{4}$$

The parameters are shape $\beta$, scale $\alpha$ and location $\xi$ which are estimated by the method of moments estimators.

### 2.4.2. Goodness-of-fit tests

We used goodness of fit tests to find the best-fitted distribution in the analysis of accurate flood frequency curves in the Geba catchment. The uncertainties of flood frequency, such as peak floods, were captured using the goodness-of-fit tests, e.g. Anderson-Darling (AD) and Kolmogorov-Smirnov (KS) tests. The GEV distribution is well fitted to the observed dataset across all the river catchments. They were processed in the EasyFit software. Using the best-fit probability type, the flood was estimated for different return periods.

*2.4.2.1. Anderson-Darling (AD) test.* The AD test compares the observed cumulative distribution function (cdf) to an expected cdf. The AD test gives more weight to the tail of the distribution than the KS test. The test hypothesis is rejected if the AD statistic is greater than a critical value of 2.5018 at the significance level $\alpha = 0.05$. The AD test statistic $A^2$ is calculated using Equation 5:

$$A^2 = -n - \frac{1}{n} \sum_{i=1}^{n} (2i-1) \left[ \ln F(xi) + \ln(1 - F(xn - i + 1)) \right] \tag{5}$$

*2.4.2.2. Kolmogorov-Smirnov (KS) test.* The KS test statistic is based on the greatest vertical distance between empirical and theoretical cdfs. Similar to the AD test statistic, a hypothesis is rejected if the KS test statistic is greater than the critical value of

0.2749 for the significance level $\alpha = 0.05$. The samples are assumed to be from a cdf $F(x)$. The test statistic $(D)$ is described in Equation 6:

$$D = \max\left[F(xi) - \frac{i-1}{n},\ \frac{i}{n} - F(xi)\right] \tag{6}$$

### 2.4.3. Flood inundation

Two-dimensional (2D) unsteady flow of hydrodynamic routing in HEC-RAS version 6.4.1 was used to produce the flood inundation, depth, and reservoir area. The 2D flow area was computed through the development of a computational grid mesh and using the developed geometric cross sections.

### 2.4.4. Hydrological drought

To characterize hydrological drought, we applied the streamflow drought index (SDI) developed by Nalbantis and Tsakiris (2009). As recommended by Diaz et al. (2016) we used a 12-month timescale, or hydrological year, to detect the evolution of hydrological drought. We characterized the hydrological drought using the variables of magnitude, duration, frequency, and severity.

According to Nalbantis and Tsakiris (2009), the SDI mathematical concept assumes a time series of monthly streamflow volume $Q_{i,j}$, where i denotes the hydrological year and j the month within that hydrological year (usually, $j = 1$ for October and $j = 12$ for September). The mathematical concept is presented in Equation 7:

$$V_{i,k} = \sum_{j=1}^{3k} Q_{i,j} \quad \mathrm{i} = 1,\ 2\ \ldots. \quad \mathrm{j} = 1, 2, \ldots\ 12 \quad \mathrm{k} = 1,\ 2, 3, 4 \tag{7}$$

where: Vi,k is the cumulative streamflow volume for the i-th hydrological year and the k-th reference period, with $k = 1$ for October–December, $k = 2$ for October–March, $k = 3$ for October–June, and $k = 4$ for October–September. Based on cumulative streamflow volumes Vi, k, the Streamflow Drought Index (SDI) is defined for each reference period k of the i-th hydrological year as follows in Equation 8:

$$SDI_{i,k} = \frac{V_{i,k} - \bar{V}_k}{S_k} \quad \mathrm{i} = 1,\ 2\ldots\ldots. \quad \mathrm{k} =\ 1,\ 2,\ 3,\ 4 \tag{8}$$

Where, Vk and Sk are respectively the mean and the standard deviation of cumulative streamflow volumes of reference period k as these are estimated over a long period of time. In this definition the truncation level is set to Vk although other values could be used. See Table 1 for the SDI classification class used in our study site.

### 2.4.5. Meteorological drought

The Standardized Precipitation Index (SPI) of the 12-month timescale was employed to assess the meteorological drought. By computing the SPI values, the study catchments were classified (Table 2). Negative SPI values below −1.0 indicate more severe

Table 1. Definition and states of hydrological drought class (Nalbantis and Tsakiris 2009).

| SN | Range | Streamflow Drought Index (SDI) class |
|---|---|---|
| 1 | SDI $\geq$ 0.0 | Non drought |
| 2 | $-1.0 \leq$ SDI $<$ 0.0 | Mild drought |
| 3 | $-1.5 \leq$ SDI $<-1.0$ | Moderate drought |
| 4 | $-2.0 \leq$ SDI $<-1.5$ | Severe drought |
| 5 | SDI $<-2.0$ | Extreme drought |

Table 2. Classification of meteorological drought by SPI (McKee et al. 1993).

| SPI | Severity |
|---|---|
| $\geq$2 | Extremely wet |
| 1.5 to 1.99 | Very wet |
| 1.0 to 1.49 | Moderately wet |
| 0.99 to 0 | Mildly wet |
| 0 to-0.99 | Mild drought |
| −1.0 to −1.49 | Moderate drought |
| −1.5 to −1.99 | Severe drought |
| $\leq$−2.0 | Extreme drought |

drought conditions, while positive SPI values indicate wetter periods or the cessation of drought. For a detailed classification, see Table 2. To represent the meteorological stations over the catchment, Atsbi station was used for Agula catchment, Wukro for Genfel catchment, and Hawzen for Suluh catchment, respectively.

### 2.4.6. Agricultural drought

The highly applicable Vegetation Condition Index (VCI) was applied for assessing vegetation stress and/or examining the response of the vegetation. Monthly eMODIS NDVI data were used as input to compute the VCI. The VCI was computed using the below Equation 9:

$$VCI = 100 * {(NDVI_i - NDVI_{\min})} \Big/ {(NDVI_{\max} - NDVI_{\min})} \tag{9}$$

Where: $NDVI_i$ = the current smoothed $NDV_I$ (Normalized Difference Vegetation Index) value of $i^{th}$ month, $NDVI_{min}$, and $NDVI_{max}$, is a minimum and maximum NDVI values for every pixel at a particular period.

VCI measures a percentile range from 0 to 100 (Kogan 1995). A high value of VCI signifies a healthy and/or unstressed vegetation condition. Thus, the area is free of agricultural drought incidence. The VCI value of 50–100% shows wet conditions or above normal. The values between 35 and 50% show an area under the incidence of moderate drought. And VCI values between 20 and 35% show a severe drought.

## 3. Results

### 3.1. Goodness-of-fit tests

In order to find the best fit for the respective rivers, the comparison of the four distribution types—GEV, Gumbel, Log-Pearson (3P), and Gamma—was analyzed (Table 3). The best-fit distribution was evaluated at the critical value $\alpha$ at 0.05 using

Table 3. Best-fit probability distributions for Suluh, Genfel, and Agula river catchments.

| | | K-S test (critical value α at 0.05 = 0.2749) | | | A-D test (critical value α at 0.05 = 2.5018) | | |
|---|---|---|---|---|---|---|---|
| Rivers | Distributions | Statistic | Reject | Rank | Statistic | Reject | Rank |
| Suluh | GEV | 0.171 | No | 1 | 4.325 | Yes | 3 |
| | Gumbel | 0.239 | No | 4 | 2.185 | No | 2 |
| | Log-Pearson (3 P) | 0.189 | No | 3 | 4.461 | Yes | 4 |
| | Gamma (3 P) | 0.174 | No | 2 | 0.925 | No | 1 |
| Genfel | GEV | 0.107 | No | 1 | 0.451 | No | 3 |
| | Gumbel | 0.211 | No | 4 | 1.409 | No | 1 |
| | Log-Pearson (3 P) | 0.153 | No | 2 | 0.575 | No | 4 |
| | Gamma (3 P) | 0.154 | No | 3 | 0.676 | No | 2 |
| Agula | GEV | 0.09278 | No | 1 | 0.21048 | No | 1 |
| | Gumbel | 0.24346 | No | 4 | 2.6423 | No | 4 |
| | Log-Pearson (3 P) | 0.12295 | No | 2 | 0.46828 | No | 2 |
| | Gamma (3 P) | 0.18418 | No | 3 | 1.0576 | No | 3 |

Anderson–Darling test (A-D), Kolmogorov–Smirnov (K-S) test.

the Anderson-Darling (A-D) and Kolmogorov-Smirnov (K-S) tests. The result showed all the distribution types were statistically accepted. The GEV distribution type was ranked first for all river catchments considered. Hence, GEV was selected as the best-fit probability distribution for the flood frequency analysis.

### 3.2. Flood frequency

The estimated flood magnitudes for 2-, 5-, 10-, 20-, 50-, and 100-year return periods at Suluh were 18.21, 19.64, 20.38, 21.15, 21.65, and 22.09 $m^3/s$, while for Genfel they were 22.94, 26.26, 27.95, 29.70, 30.78, and 31.73 $m^3/s$ for the same return periods. Similarly, for Agula, the estimated flood magnitudes for the same return periods were 37.87, 40.37, 41.41, 42.33, 42.82, and 43.19 $m^3/s$. The flood frequency curves for the three river catchments are depicted in Figure 3. Generally, the estimated flood magnitude shows an increasing trend across the return periods in all the river catchments. Comparatively, the highest flood magnitude was recorded in Agula, then Genfel, and then Suluh for all return periods. The flood magnitude of Agula is twice that of Suluh.

### 3.3. Flood inundation

The source for the reservoir is the headwater river catchments of Suluh, Genfel, and Agula. The reservoir inundated up to 12.8 $km^2$ of area at a maximum elevation of 1830 m above sea level, and the maximum water depth reached up to 80 m (see Figure 4). We computed the maximum amount of water stored in the Gereb-Geba reservoir. The reservoir has a maximum storage capacity of 363,623,063 $m^3$ at a spill-way elevation of 1830 m.a.s.l.

### 3.4. Characterization of drought

#### 3.4.1. Hydrological drought

The streamflow drought index (SDI) for each one of the three river catchments is shown in Figures 5–7. The legend denotes the streamflow drought index (SDI) values

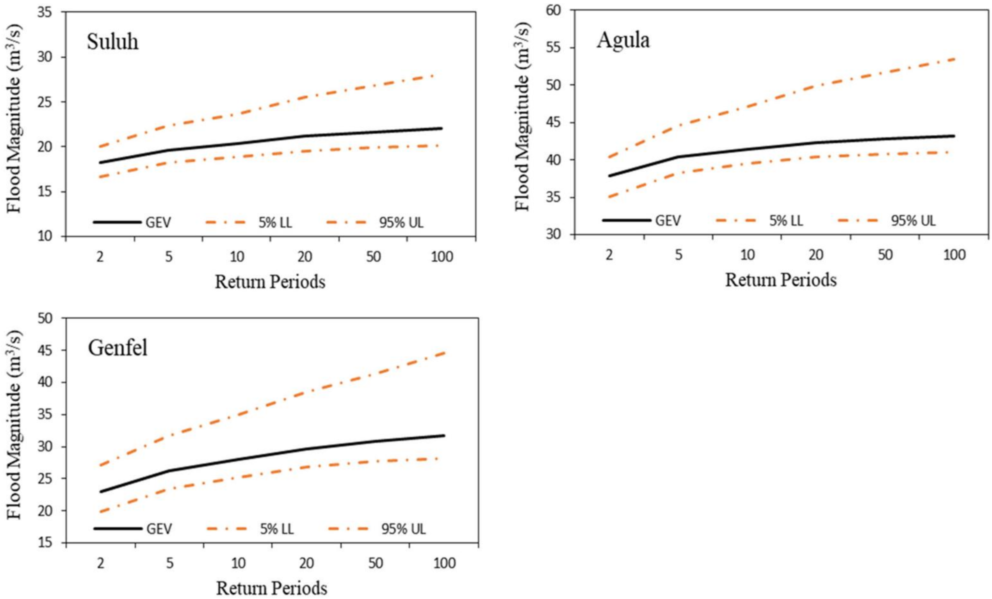


Figure 3. Estimated flood magnitude for the Suluh, Genfel, and Agula rivers versus the return periods.

with color, where deep blue indicates no drought manifestation, while red represents hydrological drought, and deep red represents extreme drought. There is high variability in SDI across river catchments. The SDI values indicate that during July and August (the rainy season), all catchments almost never show a drought signature, while drought conditions are clear during the dry months. Genfel and Suluh, but not Agula, experienced hydrological droughts for several years. The calculated onset, cessation, magnitude, duration, severity, and frequency of the drought are presented in Tables 4–6. Suluh shows a severe drought occurrence (1.66) in August 2001, which persisted for eight months (August 2001 to March 2002) (Table 4). This same hydrological drought occurred seven other times. Similarly, extreme drought was observed in April 2001 and July 2012. In particular, a hydrological drought similar to that of April 2001 has occurred three times, lasting for almost four months. For example, June 2012 witnessed a severe drought event (SDI = 1.83), with a magnitude of 1.83 lasting for one month. This was a one-time event. Notably, during April 2001, an extreme drought (SDI= 2.35) was observed with a magnitude of 9.41 and happened four times. The drought lasted for four months. Similarly, in July 2012, an extreme drought (2.13) was detected with a magnitude of 2.13 and lasted for one month. This event was again a one-time occurrence.

Similarly, Genfel also showed a mild to moderate hydrological drought class (Table 5). The mild drought was perceived in August 2001 and lasted from August 2001 to January 2005. A moderate drought was clearly noted in October 1995. During this specific year, the hydrological drought continued for ten months (October 1995 to June 1996) and frequently occurred seven times from 1992 to 2014. Figures 5–7 illustrate the extent of the hydrological drought over time series and months for the respective rivers. There is high variability in the SDI in the river

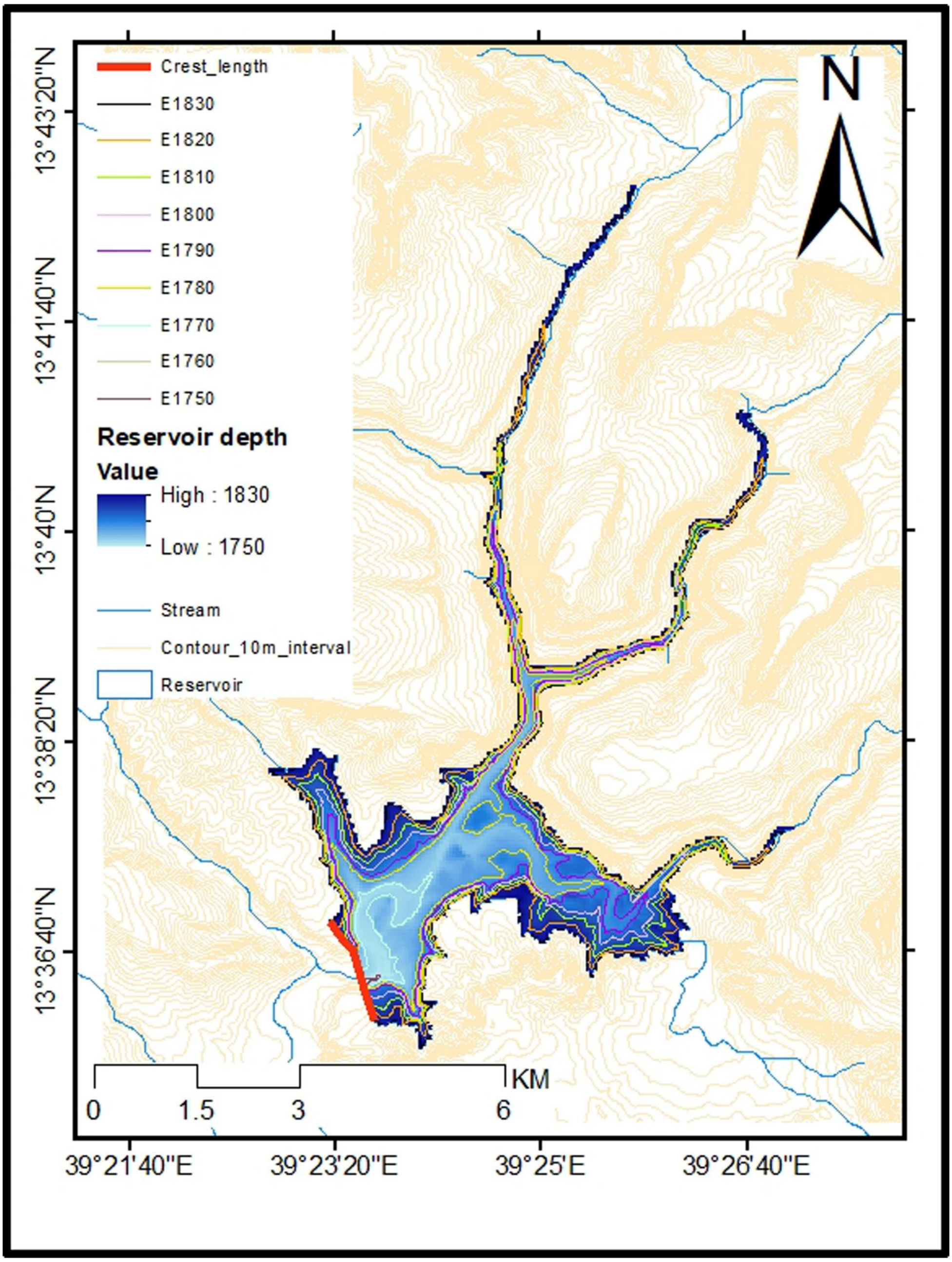


Figure 4. Flood inundation map of the Gereb-Geba reservoir.

catchments. The SDI values indicate that during July and August (the rainy season), almost all catchments did not show drought signatures, while they were well noticed during the dry months. Accordingly, Figure 5 shows the Suluh River, where the light yellow, green, and deep red colors are at their most dominant. This notion implies mild to severe drought types were commonly observed over the study period, particularly in 1990-1994, 2003-2005, and 2011/12. Typically, this type of drought was

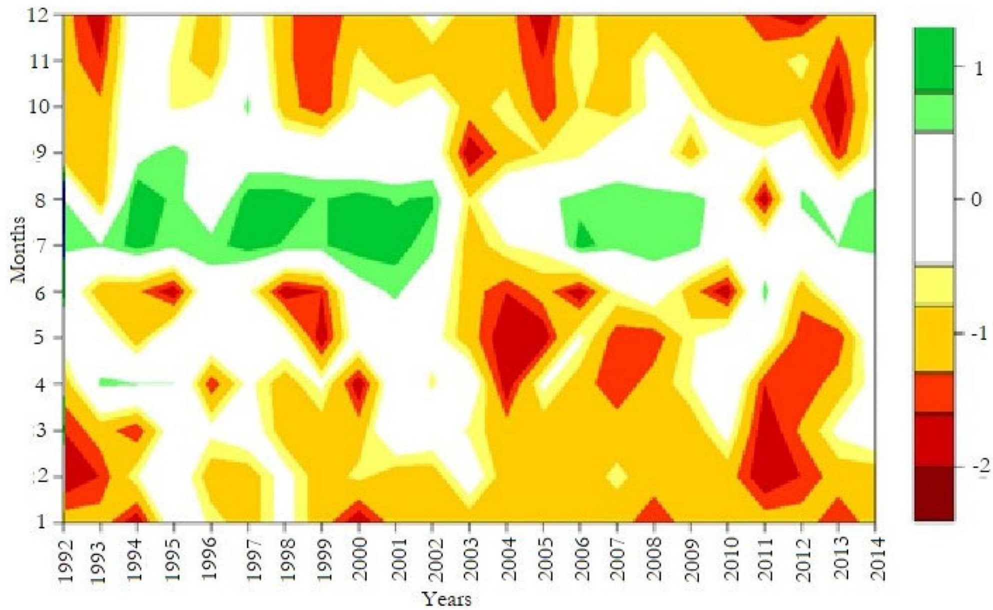


Figure 5. The temporal extent of the hydrological drought over each month in the Suluh river catchment.

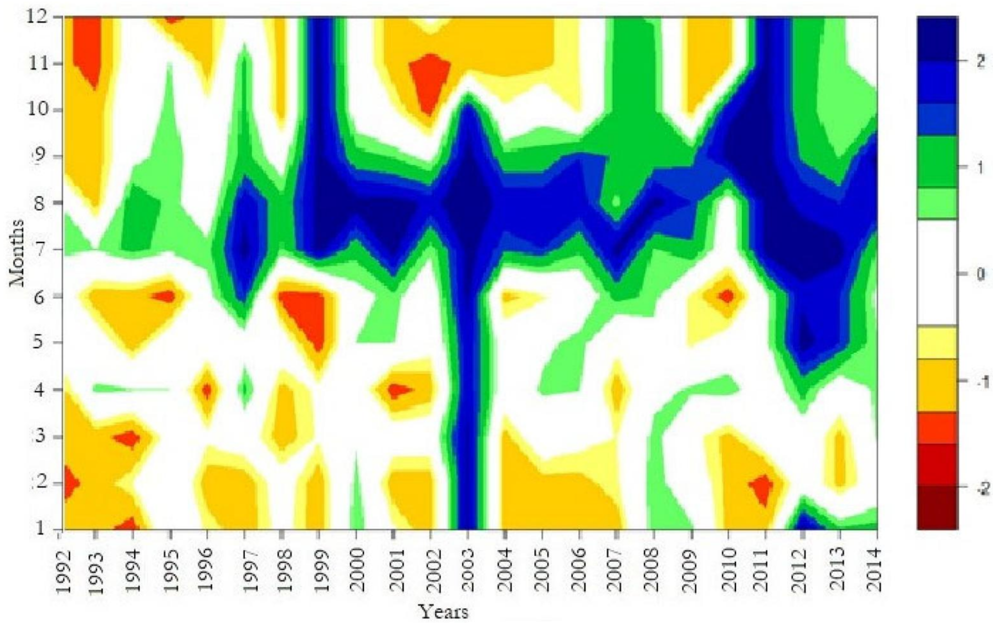


Figure 6. The temporal extent of the hydrological drought over each month in the Genfel river catchment.

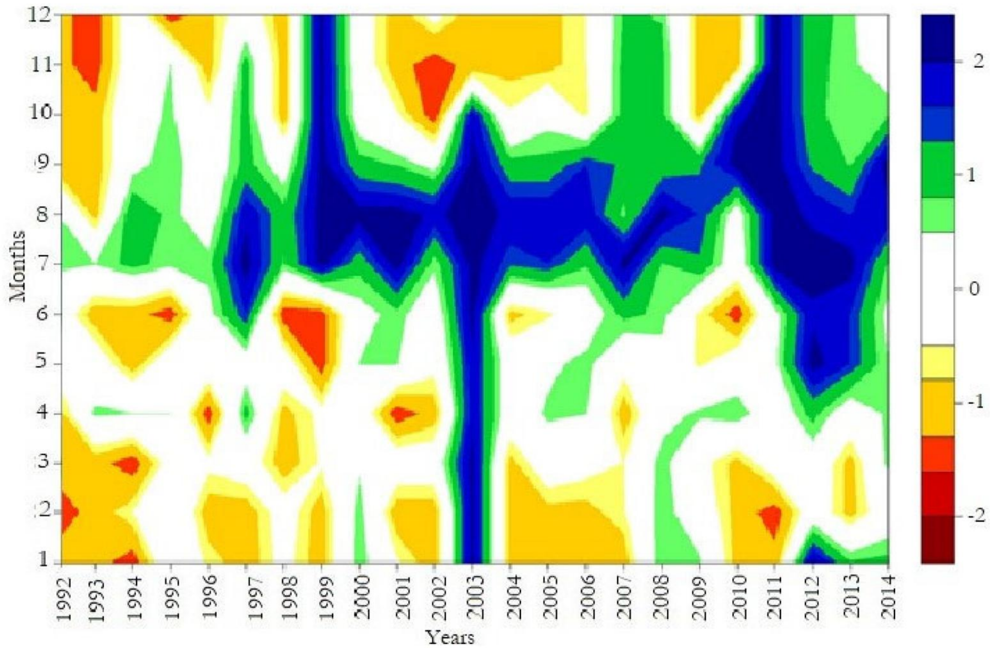


Figure 7. The temporal extent of the hydrological drought over each month in the Agula river catchment.

Table 4. Characterization of the hydrological drought in the Suluh river catchment.

| Drought class | Onset | Cessation | Duration (month) | Magnitude mm/month | Severity | Frequency (%) |
|---|---|---|---|---|---|---|
| Mild | Jun-94 | Jun-94 | 1 | 0.13 | 0.13 | 0.93 |
| | Aug-00 | Aug-00 | 1 | 0.97 | 0.97 | 0.93 |
| | Jul-03 | Jul-03 | 1 | 0.06 | 0.06 | 0.93 |
| | Jul-04 | Jun- 05 | 11 | 2.32 | 0.21 | 10.28 |
| | Jul-06 | Jul-06 | 1 | 0.02 | 0.02 | 0.93 |
| | Dec-06 | Dec-06 | 1 | 0.03 | 0.03 | 0.93 |
| | Jul-07 | Jul-08 | 12 | 6.53 | 0.54 | 11.21 |
| | Jun-09 | Jul- 09 | 2 | 0.46 | 0.23 | 1.87 |
| | Dec-09 | Dec-09 | 1 | 0.03 | 0.03 | 0.93 |
| | Jul-10 | May-12 | 23 | 12.53 | 0.54 | 21.5 |
| | Nov-12 | Oct-13 | 12 | 9.59 | 0.8 | 11.21 |
| | Jan-14 | Jul-14 | 1 | 4.04 | 4.04 | 0.93 |
| Moderate | Sep-00 | Nov-00 | 3 | 3.99 | 1.33 | 2.8 |
| | Jan-01 | Jan-01 | 1 | 1.45 | 1.45 | 0.93 |
| | Apr-02 | Jun-02 | 3 | 3.92 | 1.31 | 2.8 |
| | Aug-02 | Nov-02 | 4 | 5.65 | 1.41 | 3.74 |
| | Jan −03 | Mar-03 | 3 | 4.42 | 1.47 | 2.8 |
| | May-03 | Jun-03 | 2 | 2.79 | 1.4 | 1.87 |
| | Aug-12 | Oct-12 | 2 | 3.42 | 1.71 | 1.87 |
| | Nov-13 | Dec-13 | 2 | 2.05 | 1.02 | 1.87 |
| Severe | Dec-00 | Dec-00 | 1 | 1.52 | 1.52 | 0.93 |
| | Feb-01 | Mar-01 | 2 | 3.27 | 1.63 | 1.87 |
| | 01-Aug | Mar-02 | 8 | 13.3 | 1.66 | 7.48 |
| | Jul-02 | Jul-02 | 1 | 1.53 | 1.53 | 0.93 |
| | Dec-02 | Dec-02 | 1 | 1.55 | 1.55 | 0.93 |
| | Apr-03 | Apr-03 | 1 | 1.52 | 1.52 | 0.93 |
| | Jun-12 | Jun-12 | 1 | 1.83 | 1.83 | 0.93 |
| Extreme | Apr-01 | Jul-01 | 4 | 9.41 | 2.35 | 3.74 |
| | Jul-12 | Jul-12 | 1 | 2.13 | 2.13 | 0.93 |

Table 5. Characterization of the hydrological drought for the Genfel river catchment.

| Drought Class | Onset | Cessation | Duration (month) | Magnitude mm/month | Severity | Frequency (%) |
|---|---|---|---|---|---|---|
| Mild | Dec-92 | Dec-92 | 1 | 0.96 | 0.96 | 0.76 |
| | Jul-95 | Sep-95 | 3 | 2.19 | 0.73 | 2.29 |
| | Jul-96 | Jul-96 | 1 | 0.44 | 0.44 | 0.76 |
| | Jan-98 | Jun-98 | 6 | 2.16 | 0.36 | 4.58 |
| | Dec-99 | Feb-00 | 3 | 1.52 | 0.51 | 2.29 |
| | Aug-01 | Jan-05 | 42 | 26.14 | 0.62 | 32.06 |
| | Jul-05 | Jul-05 | 1 | 0.29 | 0.29 | 0.76 |
| | Sep-05 | Sep-05 | 1 | 0.01 | 0.01 | 0.76 |
| | Feb-06 | Jun-07 | 17 | 6.84 | 0.4 | 12.98 |
| | Oct-07 | Jul-08 | 10 | 5.66 | 0.57 | 7.63 |
| | Jun-11 | Dec-11 | 7 | 1.52 | 0.22 | 5.34 |
| | Jun-14 | Dec-14 | 7 | 1.52 | 0.22 | 5.34 |
| Moderate | Jan-93 | Jun-93 | 6 | 7.33 | 1.22 | 4.58 |
| | Aug-93 | Aug-93 | 1 | 1.42 | 1.42 | 0.76 |
| | Apr-94 | Jun-94 | 3 | 3.72 | 1.24 | 2.29 |
| | Oct-95 | Jun-96 | 10 | 11.97 | 1.2 | 7.63 |
| | Aug-99 | Nov-99 | 1 | 4.6 | 4.6 | 0.76 |
| | Jul-07 | Sep-07 | 3 | 3.81 | 1.27 | 2.29 |
| Severe | Jul-93 | Jul-93 | 1 | 1.54 | 1.54 | 0.76 |
| | Sep-93 | Mar-94 | 7 | 11.77 | 1.68 | 5.34 |

Table 6. Characterization of the hydrological drought for the Agula river catchment.

| Drought class | Onset | Cessation | Duration (month) | Magnitude mm/month | Severity | Frequency (%) |
|---|---|---|---|---|---|---|
| Mild | Dec-92 | Jul-93 | 8 | 2.70 | 0.34 | 7.27 |
| | Sep-93 | Dec-93 | 4 | 3.73 | 0.93 | 3.64 |
| | Feb-94 | Mar-94 | 2 | 1.95 | 0.97 | 1.82 |
| | Aug-94 | Aug-94 | 1 | 0.41 | 0.41 | 0.91 |
| | Jul-04 | Jul-04 | 1 | 0.06 | 0.06 | 0.91 |
| | Sep-04 | Jul-05 | 11 | 9.10 | 0.83 | 10.00 |
| | Sep-08 | Jul-13 | 58 | 45.40 | 0.78 | 52.73 |
| | Sep-13 | Jun-14 | 10 | 8.76 | 0.88 | 9.09 |
| | Sep-14 | Dec-14 | 4 | 3.05 | 0.76 | 3.64 |
| Moderate | Aug-93 | Aug-93 | 1 | 1.09 | 1.09 | 0.91 |
| | Jan-94 | Jan-94 | 1 | 1.01 | 1.01 | 0.91 |
| | Apr-94 | Jul-94 | 4 | 4.18 | 1.04 | 3.64 |
| | Aug-04 | Aug-04 | 1 | 1.05 | 1.05 | 0.91 |
| | Jul-13 | Aug-13 | 2 | 2.21 | 1.11 | 1.82 |
| | Jul-14 | Aug-14 | 2 | 2.09 | 1.05 | 1.82 |

exhibited in the dry months of October to January and was also well detected from February to May.

As depicted in Figure 6, the Genfel River, almost represented by the blue color, shows no drought occurrences, especially from 1997 to 2014. Mild to moderate drought types were observed in some years, such as 1990, 1993, and 2002. This was manifested in the dry months.

Figure 7 and Table 6 describes the Agula River. The deep blue color represents no drought at the study site. As presented in Figure 7, the deep blue color dominates the Agula River. The deep blue color is fully concentrated from June to September, especially from 1994 to 2008.

We tried to see the SDI values across the Agula, Genfel, and Suluh river catchments (Figure 8). The boxplot median value showed that the Suluh river was severely

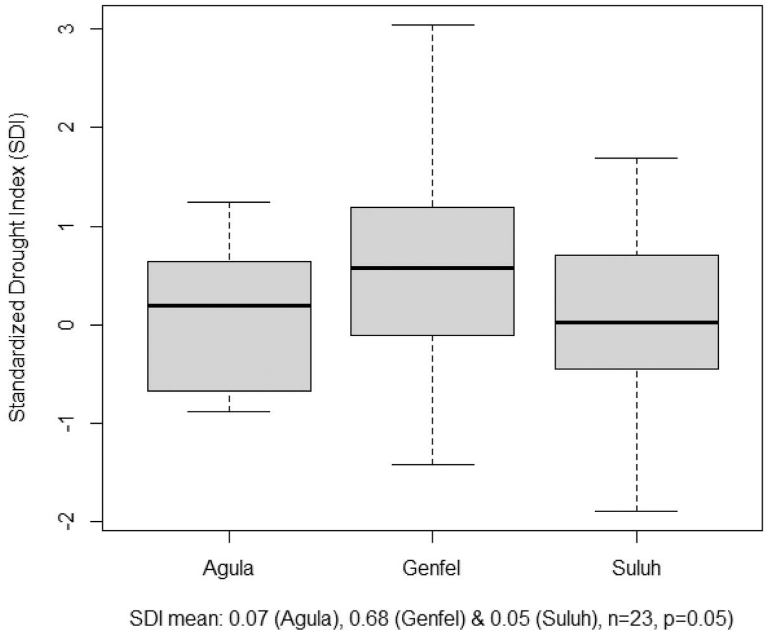


Figure 8. Annual timescale hydrological drought of Agula, Genfel, and Suluh catchments (1992–2014).

affected by hydrological drought with SDI value about less than 0, whereas Genfel and Agula were less affected by hydrological drought (SDI values $\geq 0.0$).

### 3.4.2. Meteorological drought

As shown in Figure 9, the Suluh catchment was severely affected by a metrological drought with SPI median value of about less than 0. In contrast, the Agula and Genfel catchments are relatively less affected by the metrological drought.

### 3.4.3. Agricultural drought

As depicted in Figure 10, a severe agricultural drought (20–35%) was detected in all the catchments. The VCI values were found to be almost the same across the river catchments.

As presented in Figures 9 and 10, the Standardized Precipitation Index (SPI), Standardized Drought Index (SDI), and the Vegetation Condition Index (VCI) at the annual time scale did not show significant differences in the mean annual values (SPI, $p$-value $= 0.99$, SDI, $p$-value $= 0.05$, and VCI, $p$-value $= 0.07$) at the 5% significance level among the Agula, Genfel, and Suluh catchments, respectively. This implies that all catchments have similar meteorological, hydrological, and agricultural drought conditions. Rather, a mild to mildly wet meteorological drought, a non-drought to mild hydrological drought, and a severe agricultural drought were observed. Overall, in 2008, 2009, and 2015, severe to extreme droughts were observed in the respective stations.

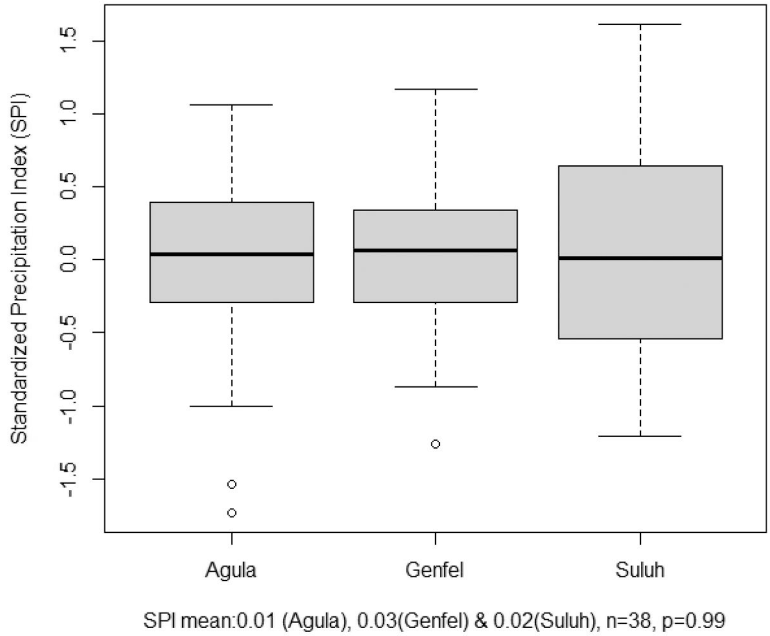


Figure 9. Annual timescale meteorological drought of Agula, Genfel, and Suluh catchments (1980–2017).

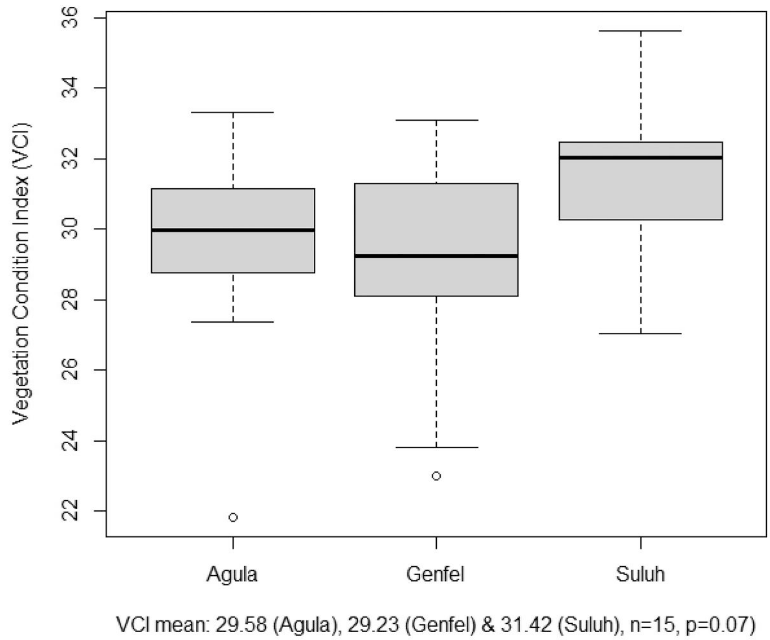


Figure 10. Annual timescale agricultural drought (VCI%) of Agula, Genfel, and Suluh catchments (2003–2017).

## 4. Discussion

### 4.1. Flood characterization

We characterized the hydrology of the headwater river catchments flowing into the Gereb-Geba water supply reservoir in the semi-arid region of the Tekeze basin, in the northern Ethiopian region of Tigray. The reservoir depends on the flow evolution of the headwaters of the Suluh, Genfel, and Agula Rivers. Flooding occurs after a prolonged rainstorm. This is common during the rainy season, from June to September. Then, a high runoff discharge occurs. The highest magnitude and peak are usually recorded in August. Table 3 shows the best good-fit and observed cumulative distribution function (CDF). We found the GEV distribution type to be the best fit in all the river catchments considered. Our result agrees with several studies conducted in African basins. For example, studies by Gilroy and McCuen (2012) and Ngongondo et al. (2011). Nobert et al. (2014) showed the GEV model performs better at fitting the frequency distribution than other distribution types. As depicted in Figure 3, the estimated flood magnitude exhibits an increasing trend across all the return periods and in all the river catchments. Usually the flood is evident in the rainy season of June to September, and the nature of the flood is intense and manifests in an instant. The Agula and Genfel river catchments have larger volumes of flood compared to the Suluh River.

Flood magnitudes for Agula, 33.5, 33.7, 33.9, and 33.9 $m^3$/s, and for Genfel, 20.8, 21.6, 22.3, and 22.6, respectively, would reoccur with 10-, 20-, 50-, and 100-year return periods, respectively. For both rivers, the highest flood magnitudes reoccur in 50- and 100-year returns, which would have the lowest probability of occurrence. Our finding is consistent with a study conducted by Zenebe et al. (2013). They reported that high flood magnitude occurs in the form of flash floods frequently during the rainy season and show an increasing trend in time in Geba subcatchments in the northern Ethiopian highlands. In addition, our result also agrees with a study conducted by Degefu et al. (2019) who found that in most of the Ethiopian basins, e.g. in Abay, Omo-Gibe, Awash, and Genalle-dawa, an increasing upward shift in floods was observed for the period 1975–2010.

The alteration of the flood magnitude is expected to be regulated to maintain the hydrological regime. It is especially important to sustain water infrastructures for their respective purposes in water-deficit semi-arid environments. Studies by Ridolfi et al. (2019) claimed that quantifying the peak flow for different return periods helps minimize different hazards related to dams and reservoirs. The large Gereb-Geba water supply dam project at the study site is expected to provide water supply for Mekelle, Tigray's capital in northern Ethiopia. The hydrological regime in the headwaters controls the management of the reservoir. The Suluh River has shown a decrease in flood magnitude, possibly attributable to the occurrence of severe and extreme hydrological droughts at the site. As a result, measures should be put in place over the catchment to maintain the hydrological regime of the river system. Our results agree with prior research. For example, Payus et al. (2020) reported that the water levels in dams on the North and Northeast Coasts of Borneo in Southeast Asia are greatly affected by the extreme droughts. It was found that the dams showed a sharp and significant drop in water level during the drought periods. Similarly, Kadir et al. (2020) also reported that the hydrological regime of the upstream part of the Medjerda River changed in the past decades. The detected hydrologic alteration will affect and reduce water availability directly, reducing it and increasing the trends in extreme events (droughts and floods). Agricultural development and irrigation are the dominant causal processes that altered the hydrological regime in the Medjerda River, Algeria. In our case, similar tendencies are also observed. The reservoir is expected to inundate an area of 12.8 $km^2$ at a maximum elevation of 1830 m with a water depth of 80 m. This has similarities with studies reported by (Desalegn and Mulu 2021; Asitatikie et al. 2022). Thus, catchment management over the rivers is important to regulate the hydrological regime of the river system. This is critical, especially in water-deficit, semi-arid environments, in order to sustain the water infrastructure's various purposes.

### 4.2. Characterization of drought

We investigated the temporal variability of the headwater river catchments using SDI, as depicted in Figures 5–7. Our findings show that the Genfel and Agula river catchments exhibit similar responses and tendencies to drought intensity, while the Suluh River responds differently, with a greater occurrence of severe to extreme drought types (Tables 4–6). The hydrological drought was described using the variables of onset, cessation, duration, magnitude, frequency, and severity of the drought in the study period (see Tables 4–6). These parameters vary across the river catchments (Tables 4–6). Mild to moderate drought types were commonly experienced in all river catchments. However, severe to extreme drought was only experienced in the Suluh River. In contrast, in the Agula and Genfel Rivers, no severe to extreme droughts were observed in the study period. As depicted in Figures 5–7, mild to severe drought types were observed in the dry (October to January) and short rainy seasons (February to May). This characteristic of the hydrological drought is common in arid or semi-arid regions. Byakatonda et al. (2018a) found that the dynamics of droughts show increasing trends in both the Limpopo and Okavango river systems, consistent with drying conditions in Botswana. And Zhang et al. (2015) also reported that a marked decrease in streamflow was observed due to drought severity, mainly in the dry season in the Huaihe River in China.

Generally, only the Suluh River showed an increasing trend in drought, while the Agula and Genfel showed less or a decreasing trend in the study period. This agrees with studies conducted in other basins. For example, Rientjes et al. (2011) reported that the low-flow index (Q95/Q50) decreased by 18.1% and 66.6% for the periods 1982–2000 and 2001–2005, respectively, in Gilgel Abbay of the upper Blue Nile basin in Ethiopia. In addition, a study in the same basin by Gebrehiwot et al. (2014) also noted a significant decreasing trend in low-flow index observed in Gilgel Abay, the upper Blue Nile basin.

In the Genfel River, despite the severe drought that occurred in July and September 1993, we detected mild to moderate drought intensity. Intrestingly, in Genfel and Agula, we perceived no severe or extreme drought event in the study period, only mild to moderate drought. In contrast, as provided in Table 4 and

Figure 5 in the Suluh, we noticed frequently severe to extreme droughts (1990-1993, 2002-2004, and 2011-2012). This implies that the hydrological regime of the Suluh River was considerably affected by the evolution of the hydrological drought episodes.

In addition, the change in streamflow might also be attributed to water management activities practiced in the catchment (Shiferaw et al. 2023). Considerable water abstraction during the dry (October to January) and short rainy seasons (February to May) for irrigation purposes has been practiced over the head catchment. Such water abstractions might aggravate the hydrological drought. This has similarities to other studies conducted in northern Ethiopia. For example, a study by Tekleab et al. (2013) showed significant decreasing trends in streamflow during the dry season (December, January, and February) in the Jedeb catchment in the upper Blue Nile basin and related them to water abstraction for irrigation purposes over the catchment. Yazew et al. (2005) also reported that storing part of the runoff in water harvesting structures for irrigation purposes reduces the downstream flow in Gumsalasa and Korir irrigation schemes. Correspondingly, Nyssen et al. (2010) reported that integrated catchment management practices reduced the overall runoff by 1.6% in the May Zeg-Zeg catchment of Tigray. Similarly, Sultan et al. (2018) also noted the impact of soil and water conservation measures across different land use and cover types, showing a 34% reduction in surface runoff volume in the Kasiry watershed in northwestern Ethiopia. Asfaw (2014) also studied the effects of climate and land use change on water resources in the Suluh catchment. He found that neither climate nor land use affect the surface runoff and baseflow in the Suluh River. This strongly supports our finding that the change in streamflow in Suluh is more pronounced due to hydrological drought effects, while Genfel and Agula experienced no drought occurrences observed over the study period. As a result, the magnitude of the Agula and Genfel floods is relatively larger than that of the Suluh River. Our findings are consistent with other studies conducted in the Ethiopian highlands (e.g. Melesse et al. 2010; Degefu et al. 2019).

Severe and extreme meteorological droughts were also observed over the study catchments. The severer droughts were observed in 2008, 2009, and 2015 across all the river catchments. This finding is in line with other studies conducted in northern Ethiopia (Gebrehiwot et al. 2011; Gidey et al. 2018; Menna et al. 2022). Relatively, the meteorological drought in Suluh was found to be higher than that in the Genfel and Agula rivers. We also perceived a severe agricultural drought (20–35%) across the river catchments. The study site is located in a semi-arid environment, and the rainfall is highly variable and mainly concentrated in July and August (Shiferaw et al. 2023). For this reason, the area is severely affected by agricultural drought.

The SPI and SDI almost showed the same pattern and were positively correlated. In contrast, a negative correlation was revealed between SDI and the VCI across the catchments. This is mainly attributed to the fact that the study catchments are located in dryland areas where rainfall is highly variable in space and time. Besides, water availability is also controlled by different catchment management systems, such as soil, geology, soil and conservation measures, water abstraction, and others. The correlation between the SDI, with SPI, and VCI was not found to be statistically significant. This is because the values of the indices across the catchments are almost homogenous.

## 5. Conclusions

This paper sought to characterize extreme events of flood and drought hazards in the headwater river catchments of the Gereb-Geba reservoir dam in the semi-arid highlands of northern Ethiopia. Managing and regulating scarce water under complex hydrological processes in semi-arid areas is crucial. The estimated flood shows increasing trends across all return periods in all three river catchments. The maximum storage capacity of the reservoir is 363 million $m^3$, and the flood inundated an area of 12.8 $km^2$ at a maximum elevation of 1830 m.a.s.l.

The Suluh River experienced severe-to-extreme hydrological drought episodes. In contrast, in Agula and Genfel, we detected no or less severe drought observations. This elucidated that the hydrological drought considerably affects the streamflow change at the study site, particularly the drought observed in the Suluh, which might have a negative impact on the Gerb-Geba reservoir. Severe to extreme meteorological drought was also detected in the Suluh, Genfel, and Agula catchments, respectively. Besides, a severe agricultural drought with a VCI value of 20–35% was perceived across the catchments.

Overall, our findings provide far-reaching implications for water resources planning and management to reduce drought and flood hazard risks. To preserve the hydrological regime of the headwater rivers, effective land and water management plans are required. Since the study site has limited and missing data records, our streamflow analysis was restricted to the 2014 period. Therefore, we further recommend that future studies reconstruct the long-missing streamflow data records of the study site. Moreover, we recommend exploring the flood and drought hazards under climate change and coming up with strategic adaptive capacity measures at local levels.

## Acknowledgments

We gratefully acknowledge the financial support provided by the Open Society Foundation (OSF)–Africa Climate Change Adaptation Initiative (ACCAI). The authors also wish to acknowledge the Ministry of Water, Irrigation and Energy (MoWIE) and the National Meteorological Agency (NMA) of Ethiopia for providing the necessary daily streamflow and rainfall data records for the study site.

## Disclosure statement

No potential conflict of interest was reported by the authors.

## Funding

We acknowledge the financial support by the Open Society Foundation (OSF)–Africa Climate Change Adaptation Initiative (ACCAI) project under [Grant No. OR2016-30576] hosted at the Institute of Climate and Society, Mekelle University (MU-ICS).

## Author contributions

All authors collaborated on the research by making the following contributions: Henok Shiferaw: conceptualization, data collection, data analysis, and manuscript drafting; Amanuel Zenebe: conceptualization, data analysis, guidance, manuscript reviewing, supervision, fund acquisition, and project administration; Eyasu Yazew: conceptualization, data analysis, manuscript reviewing, guidance and supervision; Biniyam Yisak: data collection, data analysis, and manuscript drafting; Atkilt Girma: data collection, data analysis, and manuscript drafting; Muez Araya: data collection, data analysis, and manuscript drafting; Gebreyohannes Zenebe: data collection, data analysis, and manuscript drafting; and Alessandra Giannini: manuscript reviewing and data analysis guidance.

## ORCID

Henok Shiferaw http://orcid.org/0000-0002-3889-4965
Amanuel Zenebe http://orcid.org/0000-0001-6571-9065
Eyasu Yazew http://orcid.org/0000-0003-2300-8681
Biniyam Yisak http://orcid.org/0000-0002-9954-4344
Atkilt Girma http://orcid.org/0000-0001-7081-9503
Alessandra Giannini http://orcid.org/0000-0001-5425-4995

## Data availability statement

The data and material used in this research are available upon request from the first author or corresponding author.

## References

Altin B, Sar F, Altin NB. 2019. Determination of drought intensity in Seyhan and Ceyhan River Basins, Turkey, by hydrological drought analysis. Theor Appl Climatol. 139:95–107. doi: 10.1007/s00704-019-02957-y.

Asfaw BA. 2014. Modeling the effect of climate and land use change on the water resources in Northern Ethiopia: the case of Suluh River basin [Dissertation]. Berlin, Germany: Freie Universität.

Asitatikie AN, Kifelew MS, Shumey EE. 2022. Flood inundation modeling using HEC-RAS: the case of downstream Gumara river, Lake Tana sub basin, Ethiopia. Geocarto Int. 37(25): 9625–9643. doi: 10.1080/10106049.2021.2022014.

Awass AA. 2009. Hydrological drought analysis-occurrence, severity, risks: the case of Wabi Shebele River Basin [Dissertation]. Germany: Forschungsinstitut Wasser und Umwelt.

Byakatonda J, Parida BP, Kenabatho PK. 2018a. Relating the dynamics of climatological and hydrological droughts in semiarid Botswana. Phys Chem Earth. 105:12–24. doi: 10.1016/j.pce.2018.02.004.

Byakatonda J, Parida BP, Moalafhi DB, Kenabatho PK. 2018b. Analysis of long term drought severity characteristics and trends across semiarid Botswana using two drought indices. Atmos Res. 213:492–508. doi: 10.1016/j.atmosres.2018.07.002.

Degefu MA, Tena A, Gete Z, Woldeamlak B. 2019. Detection of trends in hydrological extremes for Ethiopian. Reg Environ Change. 19(7):1923–1933. doi: 10.1007/s10113-019-01510-x.

Desalegn H, Mulu A. 2021. Mapping flood inundation areas using GIS and HEC-RAS model at Fetam River, Upper Abbay Basin, Ethiopia. Sci African. 12:e00834. doi: 10.1016/j.sciaf.2021.e00834.

Diaz V, Corzo G, Solomatine D, Van HAJ. 2016. Spatio-temporal analysis of hydrological drought at catchment scale using a spatially-distributed hydrological model. Procedia Eng. 154:738–744. doi: 10.1016/j.proeng.2016.07.577.

Ekolu J, Dieppois B, Sidibe M, Eden JM, Tramblay Y, Villarini G, Peña-Angulo D, Mahé G, Paturel J-E, Onyutha C, et al. 2022. Long-term variability in hydrological droughts and floods in Sub-Saharan Africa: new Perspectives from a 65-year daily streamflow dataset Original citation. J Hydrol. 613:128359. doi: 10.1016/j.jhydrol.2022.128359.

Ridolfi E, Di Francesco S, Pandolfo C, Berni N, Biscarini C, Manciola P. 2019. Coping with extreme events: Effect of Different reservoir operation strategies on flood inundation maps. Water. 11:1–18. doi: 10.3390/w11050982.
Gebrechorkos SH, Hülsmann S, Bernhofer C. 2019. Long-term trends in rainfall and temperature using high-resolution climate datasets in East Africa. Sci Rep. 9(1):11376. doi: 10.1038/s41598-019-47933-8.
Gebrechorkos SH, Taye MT, Birhanu B, et al. 2023. Future changes in climate and hydroclimate extremes in East Africa Earth's future. 11:1–21. doi: 10.1029/2022EF003011.
Gebrehiwot SG, Gärdenäs AI, Bewket W, Seibert J, Ilstedt U, Bishop K. 2014. The long-term hydrology of East Africa's water tower: statistical change detection in the watersheds of the Abbay Basin. Reg Environ Change. 14(1):321–331. doi: 10.1007/s10113-013-0491-x.
Gebrehiwot T, Van Der VA, Maathuis B. 2011. Spatial and temporal assessment of drought in the Northern highlands of Ethiopia. Int J Appl Earth Obs Geoinf. 13(3):309–321. doi: 10.1016/j.jag.2010.12.002.
Gebremeskel Haile G, Tang Q, Sun S, Huang Z, Zhang X, Liu X., 2019. Droughts in East Africa: causes, impacts and resilience. Earth-Science Rev. 193:146–161. doi: 10.1016/j.earscirev.2019.04.015.
Gebremicael TG, Mohamed YA, Van der Zaag P. 2019. Attributing the hydrological impact of different land use types and their long-term dynamics through combining parsimonious hydrological modelling, alteration analysis and PLSR analysis. Sci Total Environ. 660:1155–1167. doi: 10.1016/j.scitotenv.2019.01.085.
Gebremicael Mohamed YA, van der Zaag P, Hagos EY. 2016. Temporal and spatial changes of rainfall and streamflow in the Upper Tekeze – Atbara River Basin, Ethiopia. Hydrol Earth Syst Sci Discuss. 21:1–29. doi: 10.5194/hess-2016-318.
Gidey E, Dikinya O, Sebego R, Segosebe E, Zenebe A. 2018. Modeling the spatio-temporal meteorological drought characteristics using the standardized precipitation index (SPI) in Raya and its environs, Northern Ethiopia. Earth Syst Environ. 2(2):281–292. doi: 10.1007/s41748-018-0057-7.
Gilroy KL, McCuen RH. 2012. A nonstationary flood frequency analysis method to adjust for future climate change and urbanization. J Hydrol. 414-415:40–48. doi: 10.1016/j.jhydrol.2011.10.009.
IPCC. 2012. Summary for policymakers. In: Field CB, Barros V, Stocker TF, Qin D, Dokken DJ, Ebi KL, Mastrandrea MD, Mach KJ, Plattner G-K, SK Allen, Tignor M, and Midgley PM. editor. Managing the risks of extreme events and disasters to advance climate change adaptation. A special report of Working Groups I and II of the intergovernmental panel on climate change. Cambridge; New York: Cambridge University Press, pp. 1–19.
Kadir M, Fehri R, Souag D, Vanclooster M. 2020. Regional studies exploring causes of streamflow alteration in the Medjerda river, Algeria. J Hydrol Reg Stud. 32:100750. doi: 10.1016/j.ejrh.2020.100750.
Kogan FN. 1995. Application of vegetation index and brightness temperature for drought detection. Adv Sp Res. 15(11):91–100. doi: 10.1016/0273-1177(95)00079-T.
Kundzewicz ZW, Kaczmarek Z. 2009. Coping with hydrological extremes. Water Int. 25(1):66–75. doi: 10.1080/02508060008686798.
Markantonis V, Farinosi F, Dondeynaz C, Ameztoy I, Pastori M, Marletta L, Ali A, Moreno CC. . 2018. Assessing floods and droughts in the Mékrou River Basin (West Africa): a combined household survey and climatic trends analysis approach. Nat Hazards Earth Syst Syst Sci. 18:1279–1296. doi: 10.5194/nhess-18-1279-2018.
Mbungu W, Ntegeka V, Kahimba FC, Taye M, Willems P., 2012. Temporal and spatial variations in hydro-climatic extremes in the Lake Victoria basin. Phys Chem Earth. 50-52:24–33. doi: 10.1016/j.pce.2012.09.002.
McKee TB, Kleis, NJD, John. 1993. The relationship of drought frequency and duration to time scales. In: The relationship of drought frequency and duration to time scales; p. 179–183.

McMartin DW, Hernani Merino BH, Bonsal B, Hurlbert M, Villalba R, Ocampo OL, Upegui JJV, Poveda G, Sauchyn DJ. 2018. Limitations of water resources infrastructure for reducing community vulnerabilities to extremes and uncertainty of flood and drought. Environ Manage. 62(6):1038–1047. doi: 10.1007/s00267-018-1104-8.
Melesse A, Abtew W, Dessalegne T, Wang X. 2010. Low and high flow analyses and wavelet application for characterization of the Blue Nile River system. Hydrol Process. 24(3):241–252. doi: 10.1002/hyp.7312.
Melo DdCD, Scanlon BR, Zhang Z, Wendland E, Yin L. 2016. Reservoir storage and hydrologic responses to droughts in the Paraná River basin, south-eastern Brazil. Hydrol Earth Syst Sci. 20(11):4673–4688. doi: 10.5194/hess-20-4673-2016.
Menna BY, Mesfin HS, Gebrekidan AG, Siyum ZG, Tegene MT. 2022. Meteorological drought analysis using copula theory for the case of upper Tekeze river basin, Northern Ethiopia. Theor Appl Climatol. 149(1–2):621–638. doi: 10.1007/s00704-022-04061-0.
Nalbantis I, Tsakiris G. 2009. Assessment of hydrological drought revisited. Water Resour Manage. 23(5):881–897. doi: 10.1007/s11269-008-9305-1.
Ngongondo CS, Xu C-Y, Tallaksen LM, Alemaw B, Chirwa T. 2011. Regional frequency analysis of rainfall extremes in Southern Malawi using the index rainfall and L-moments approaches. Stoch Environ Res Risk Assess. 25(7):939–955. doi: 10.1007/s00477-011-0480-x.
NMA. 2021. Ethiopia National Meteorological Agency station data service. Addis Ababa, Ethiopia: NMA.
Nobert J, Mugo M, Gadain H. 2014. Estimation of design floods in ungauged catchments using a regional index flood method. A case study of Lake Victoria Basin in Kenya. Phys Chem Earth. 67–69:4–11. doi: 10.1016/j.pce.2014.02.001.
Nyssen J, Clymans W, Descheemaeker K, Poesen J, Vandecasteele I, Vanmaercke M, Zenebe A, Van Camp M, Haile M, Haregeweyn N, et al. 2010. Impact of soil and water conservation measures on catchment hydrological response a case in north Ethiopia. Hydrol Process. 24(13):1880–1895. doi: 10.1002/hyp.7628.
Payus C, Ann Huey L, Adnan F, Besse Rimba A, Mohan G, Kumar Chapagain S, Roder G, Gasparatos A, Fukushi K. 2020. Impact of extreme drought climate on water security in North Borneo: case study of Sabah. Water. 12(4):1135. doi: 10.3390/w12041135.
Rientjes THM, Haile AT, Kebede E, Mannaerts CMM, Habib E, Steenhuis TS. 2011. Changes in land cover and stream flow in Gilgel Abbay catchment, upper Blue Nile basin Ethiopia. Hydrol Earth Syst Sci. 15(6):1979–1989. doi: 10.5194/hess-15-1979-2011.
Salinas JL, Castellarin A, Kohnová S, Kjeldsen TR. 2014. Regional parent flood frequency distributions in Europe–Part 2: climate and scale controls. Hydrol Earth Syst Sci. 18(11): 4391–4401. doi: 10.5194/hess-18-4391-2014.
Seyoum M, van Andel SJ, Xuan Y, Amare K. 2013. Precipitation forecasts for rainfall runoff predictions. A case study in poorly gauged Ribb and Gumara catchments, upper Blue Nile, Ethiopia. Phys Chem Earth. 61-62:43–51. doi: 10.1016/j.pce.2013.05.005.
Shiferaw H, Gebremedhin A, Gebretsadkan T, Zenebe A. 2018. Modelling hydrological response under climate change scenarios using SWAT model: the case of Ilala watershed, Northern Ethiopia. Model Earth Syst Environ. 4(1):437–449. doi: 10.1007/s40808-018-0439-8.
Shiferaw H, Girma A, Hadush K, Mariam HG, Yazew E, Zenebe A. 2023. Long - term hydro-climatic variability over the semi - arid Ethiopian highlands in relation to ENSO and IOD teleconnection signals. Theor Appl Climatol. 153(1–2):193–211. doi: 10.1007/s00704-023-04450-z.
Sultan D, Tsunekawa A, Haregeweyn N, Adgo E, Tsubo M, Meshesha DT, Masunaga T, Aklog D, Fenta AA, Ebabu K. 2018. Impact of soil and water conservation interventions on watershed runoff response in a tropical humid highland of Ethiopia. Environ Manage. 61(5):860–874. doi: 10.1007/s00267-018-1005-x.
Tabari H. 2020. Climate change impact on flood and extreme precipitation increases with water availability. Sci Rep. 10(1):13768. doi: 10.1038/s41598-020-70816-2.

Tallaksen LM, Van Lanen HAJ. 2004. Hydrological drought: processes and estimation methods for streamflow and groundwater. Amsterdam, Netherlands: Elsevier.

Tekleab S, Mohamed Y, Uhlenbrook S. 2013. Hydro-climatic trends in the Abay/Upper Blue Nile basin, Ethiopia. Phys Chem Earth. 61–62:32–42. doi: 10.1016/j.pce.2013.04.017.

Tesfaye S, Birhane E, Leijnse T, Zee, S, Van Der. 2017. Climatic controls of ecohydrological responses in the highlands of northern Ethiopia. Sci Total Environ. 609:77–91. doi: 10.1016/j.scitotenv.2017.07.138.

Wang H, Zhou J, Tang Y, Liu Z, Kang A, Chen B., 2020. Flood economic assessment of structural measure based on integrated flood risk management: a case study in Beijing. J Environ Manage. 280:111701. doi: 10.1016/j.jenvman.2020.111701.

Wilhite D. 2000. Drought: a global assessment. Abingdon, Oxon: Routledge.

World Economic Forum. 2017. Global risks 2017: A global risk network report. Geneva: World Economic Forum.

Yazew E, Schiltz B, Haile M. 2005. Development and management of irrigated lands in Tigray, Ethiopia [PhD Dissertation]. The Netherlands: UNESCO-IHE.

Yin J, Gentine P, Slater L. 2023. Future socio-ecosystem productivity threatened by compound drought–heatwave events. Springer US.

Yin J, Guo S, Gentine P, Sullivan SC, Gu L, He S, Chen J, Liu P. 2021. Does the hook structure constrain future flood intensification under anthropogenic climate warming? Water Resour Res. 57(2):1–22. doi: 10.1029/2020WR028491.

Yin J, Guo S, Yang Y, Chen J, Gu L, Wang J, He S, Wu B, Xiong J. 2022. Projection of droughts and their socioeconomic exposures based on terrestrial water storage anomaly over China. Sci China Earth Sci. 65(9):1772–1787. doi: 10.1007/s11430-021-9927-x.

Zenebe A, Vanmaercke M, Poesen J, Verstraeten G, Haregeweyn N, Haile M, Amare K, Deckers J, Nyssen J. 2013. Spatial and temporal variability of river flows in the degraded semi-arid tropical mountains of northern Ethiopia. zfg. 57(2):143–169. doi: 10.1127/0372-8854/2012/0080.

Zhang R, Chen X, Zhang Z, Shi P. 2015. Evolution of hydrological drought under the regulation of two reservoirs in the headwater basin of the Huaihe River, China. Stoch Environ Res Risk Assess. 29(2):487–499. doi: 10.1007/s00477-014-0987-z.

Zhang Q, Gu X, Singh VP, Xiao M. 2014. Flood frequency analysis with consideration of hydrological alterations: Changing properties, causes and implications. J Hydrol. 519:803–813. doi: 10.1016/j.jhydrol.2014.08.011.